# RF neutron spin flippers in time of flight Spin-Echo Resolved Grazing Incidence Scattering (SERGIS)

Parnell, S. R.; Dalgliesh, R. M.; Steinke, N. J.; Plomp, J.; Van Well, A. A.

**DOI**
10.1088/1742-6596/1021/1/012040

**Publication date**
2018

**Document Version**
Final published version

**Published in**
Journal of Physics: Conference Series

# RF neutron spin flippers in time of flight Spin-Echo Resolved Grazing Incidence Scattering (SERGIS)

IOP Conf. Series: Journal of Physics: Conf. Series **1021** (2018) 012040 doi:10.1088/1742-6596/1021/1/012040

# RF neutron spin flippers in time of flight Spin-Echo Resolved Grazing Incidence Scattering (SERGIS)

**S.R.Parnell**

Faculty of Applied Sciences, Delft University of Technology, Mekelweg 15, 2629 JB Delft, The Netherlands

**R.M.Dalgliesh, N.J.Steinke**

ISIS Neutron Source, Rutherford Appleton Laboratory, Chilton, Didcot, Oxfordshire, OX11 0QX, United Kingdom

**J.Plomp, A.A. Van Well**

Faculty of Applied Sciences, Delft University of Technology, Mekelweg 15, 2629 JB Delft, The Netherlands

**Abstract.** RF coils have been routinely used for Larmor labelling on the Offspec instrument at ISIS. These coils encode directional information via the neutron polarization using a series of parallelogram-shaped pole shoes which can be tuned to different angles with an RF gradient flipper in the centre of each magnet. We report on measurements of the magnetic field integral through the coils in reflection geometry for a range of scattering angles and different pole shoe angles. Such information is mapped out by measuring the phase of the neutron polarisation and the measurements are discussed in light of data on patterned silicon gratings with a dewetted polymer and the visibility of in-plane structures to SERGIS.

## 1. Introduction

In typical neutron scattering experiments information on the sample under investigation is obtained via measurement of the momentum transfer (Q) and/or the energy change of the neutron. Efforts to increase the resolution both in scattering angle and energy often result in tight beam collimation which is wasteful in terms of the usable neutron flux. Alternative techniques have been around for several decades now [1, 2, 3] which utilise magnetic fields to manipulate the neutron spin by encoding either the scattering angle or the energy transfer in the neutron polarisation. Scattering angle encoding involves shaped magnetic fields such that the accumulated Larmor precession is dependent upon the spatial trajectory of the neutron. A number of different technologies have been developed for such spatial encoding such as magnetised thin films [4], resistive shaped magnets [5, 6], superconducting coils [7, 8, 9] and RF coils which can be either tilted [2] or utilise shaped pole pieces [10].

For scattering angle encoding applications in SANS the Spin-Echo Small Angle Neutron Scattering (SESANS) [3] technique has been applied to measure 100's of nm's to micron size structures in for example soft matter [11], granular media [12] and food [13]. The high resolution

obtained in Larmor diffraction [14] allows changes in lattice spacings $\left(\frac{\Delta d}{d}\right)$ of the order $10^{-6}$ to be measured [15] .

However the Larmor labelling analogue in reflectometry, Spin-Echo Resolved Grazing Incidence Scattering (SERGIS) [16, 17] has only, with two exceptions, been successful in measuring well-defined periodic structures. For example, silicon gratings with ridges parallel to the neutron beam [18, 19]. In the two cases of non-periodic structures, Parnell *et al.* [20] looked at the formation of crystallites in a solar cell material on a silicon layer, showing that these were detectable after annealing and verified this with microscopy. This was performed on the instrument Offspec at ISIS [10]. At ILL on the Eva instrument Vorobiev *et al.* [21] looked at a dewetted polymer on a silicon substrate. They observed features in the SERGIS signal, which were attributed to in-plane correlations between the dewetted polymer islands and agreed well with microscopy measurements. They were able to obtain good signal to noise by measuring in the Yoneda region which enhances the scattering by a factor of four [22]. However, attempts to perform such measurements at ISIS on the Offspec instrument have thus far been unsuccessful.

One of the intrinsic problems of the SERGIS technique is the following. Analogously to spin-echo SANS (SESANS), where the spin-echo (SE) signal from the in-plane structures is hidden in the direct beam intensity, the SE-signal in SERGIS is superimposed on the specular intensity and the measured polarisation ($P_{se}$) is dominated by the reflected intensity from the specular component ($I_r$) and the diffuse component ($I_d$), given by $P_{se} = (I_d P_d + I_r P_0)/(I_d + I_r)$ with $P_0$ the polarisation of the reference beams and $P_d$ the diffuse beams.

In a SESANS experiment the SE-signal can be enhanced by using thicker samples. Unfortunately, in SERGIS this enhancement is limited since the scattering volume in films is by definition small. However, the relative SE-signal in the off-specular scattering might be larger. But here we run into another problem. Whereas the SERGIS technique yields information of in-plane structures on the tens or hundreds of nm scale, detectable off-specular intensity occurs if there is in-plane structure on the micron scale, limiting the technique to samples exhibiting inhomogeneities on a broad range of length scales. A remedy to cope with these limitations could be by making a substrate having artificial in-plane structure on the micron scale, i.e. a grating and deposit the system under study onto this substrate. This creates scattering, however being on the micron range this should not add confinement effects or any perturbation upon structures on the order of the 10 nm range.

Spin-echo techniques rely on the exact cancelling of the field integral in the first arm by that of the second arm. Aberrations as a result of the different trajectories present in the experiment will lead to precession phase errors. The structure of the remainder of these proceedings is as follows. We first define a procedure to map out the phase as a function of scattering angle. Secondly we use this known phase in the determination of the polarisation ($P_{se}$) from a bare structured grating and also one onto which a dewetted polymer has been placed.

## 2. RF Coil layout and configuration for SERGIS

The schematic of figure 1 (a) is a generalised version of scattering angle encoding. The shaped field regions perform the angle encoding and are arranged with opposite magnetic field, in the case of an unscattered neutron it traverses both magnetic fields and the Larmor phase added in the first magnet is cancelled by the second magnet for all possible angles $\phi_i$. Whereas if it is scattered the resulting path difference results in a different Larmor phase which varies with the strength of the magnet and the degree of scattering is measured in the change in $P_{se}$. As discussed in [10] the same Lamor phase encoding can be achieved using a series parallelogram-shaped precession regions with flippers in the centre of each magnet. Such a setup is shown in 1 (c) both top and side view. The scattering geometry (defined in figure 1 (b)) is such that the SERGIS encoding is along the $Q_y$ direction, as reflectometry use a letter box shaped beam then there is normally no resolution along this direction and it only via SERGIS that this resolution

is obtained.

As illustrated in the side view in figure 1 (c) the path through the magnetic fields along the scattered arm vary with angle ($\theta_f$). Hence the field integral changes. In order to correct for these changes we have developed a procedure which is detailed in the following section. As the length scales $\delta_{se}$ (termed the spin echo length) probed vary with the neutron wavelength ($\lambda$) and the magnet angle ($\theta_0$) as $\delta_{se} = c\lambda^2 BLcot\theta_0/(2\pi)$ where B is the magnetic field strength, L is the separation between the magnets (see figure 1(c)) and $c = \gamma m/h = 4.632 \times 10^{14} T^{-1} m^{-2}$). Then it is necessary to correct for these integral changes as a function of $\lambda$, $\theta_0$ and $\theta_f$.

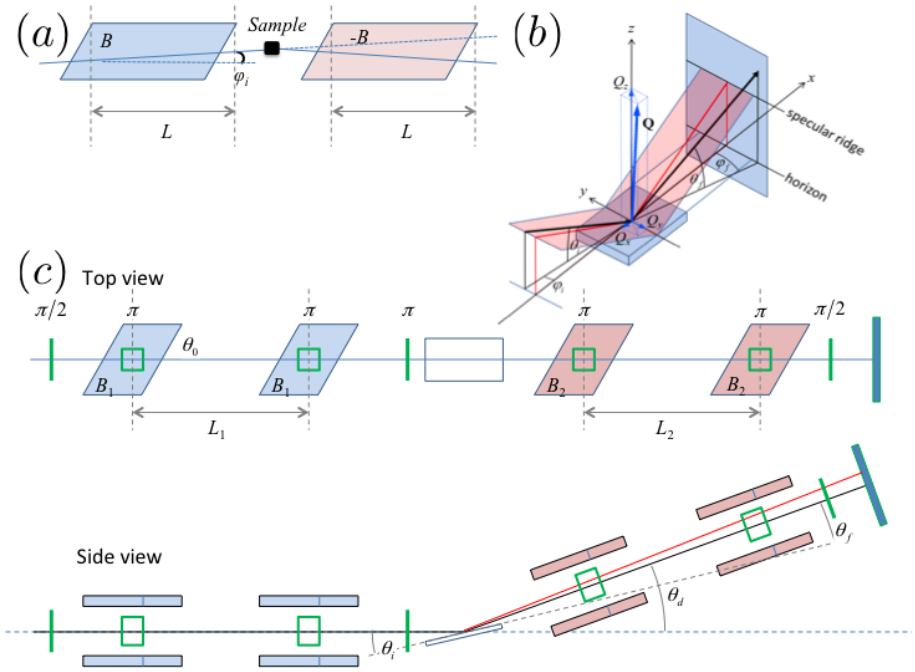


**Figure 1.** Schematic drawing showing an idealised case of scattering angle encoding in (a). In (b) the reflection geometry, illustrating the reference Cartesian co-ordinate system, the scattering vector Q and its coordinates as well as the angles $\theta$ and $\phi$ and (c) the layout of the spin encoding coils. In all cases the shaded regions indicate the magnetic field regions with changes from blue to red reflecting opposite magnetic field directions.

## 3. Measurement of the field integral as a function of scattering angle

To correct for such effects it is necessary to measure a series of polarisation echos on the detector and then to measure these over a range of $\theta_f$ values. This is the same procedure that was first used by Farago [23] for inelastic time of flight spin echo. Note that in order to avoid ambiguity we refer to the polarisation $P(\lambda)$ as the polarisation measured at a particular point whilst the echo polarisation, $P_0(\lambda)$is the maximum achievable polarisation when the echo is balanced.

The experiments were performed on the Offspec instrument at the ISIS Pulsed Neutron Source, UK. In these measurements we used a non-polarising supermirror (m=5) and measured the polarisation at different glancing angles $\phi$ for a fixed detector angle $\theta_d$. The spin-echo polarisation for specular reflection occurs at an angle $\theta_f = 2\phi - \theta_i$, where $\theta_i$ is the incident angle and $\phi$ the glancing angle given by;

$$P(\lambda) = P_0(\lambda) cos\left(\frac{\gamma m}{h}\lambda\left(2B_1L_1 - 2B_2L_2\right)\right) \quad (1)$$

with $2BL$ being the effective magnetic field integral from the arms before and after the sample (as denoted by the subscripts), with the factor of 2 occurring due to the use of RF. This can be parameterised in terms of a current applied to the correction coil ($I_{scan}$) and we denote the current at which the echo is balanced in the straight through beam as $I_0$ and an offset current which varies as a function of reflection angle ($\theta_f$), hence this becomes;

$$P\left(\lambda, I_{Scan}, \theta\right) = P_0(\lambda) cos\left(c\lambda\left(I_{scan} - I_0 - \Delta_I(\theta_f)\right)\right) \quad (2)$$

From the contour plots in figure 2 one period for $\lambda = 0.68nm$ corresponds to a change in current ($\Delta I_{scan}$) of 0.85 A. Hence as $\gamma m/h\lambda Bl = 2\pi$ (i.e. one rotation) then the change in field integral of 0.85A is $\Delta(BL) = 2\times10^{-5}Tm$, hence a change in the scan current of 1 A corresponds to $\Delta(BL) = 2.4\times10^{-5}Tm$.

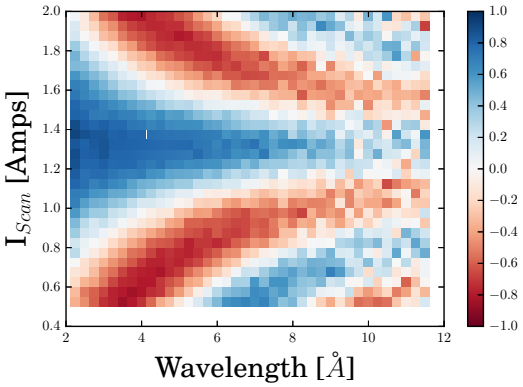


**Figure 2.** False colour plot of the polarisation as a function of wavelength for different values of the correction coil applied current $I_{scan}$ for the m=5 supermirror at a glancing angle of 0.35° and a pole shoe angle of 50° with the side bar indicating the value of polarisation.

In order to extract the echo polarisation we fit for each wavelength (0.15 Åwide bins) to equation 2. This allows the determination of the echo polarisation as a function of reflection angle. From figure 2 we determine that the echo current is independent of wavelength at 1.3A, which is to be expected and hence we can parameterise this for all wavelengths, we can also quantify this offset for various pole shoe angles (see figure 3). In summary these measurements show that the phase varies in a predictable manner and can be parameterised.

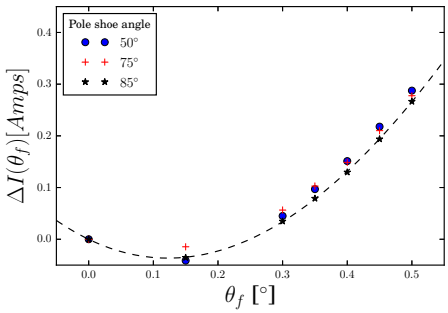


**Figure 3.** Field integral offset current ($\Delta_I(\theta_f)$) for measurements with the m=5 supermirror as a function of reflection angle.

## 4. Field integral correction in SERGIS example

The sample under investigation was a block co-polymer made of deuterated polystyrene and paramethylstyrene [24]. Grazing Incidence Small Angle Neutron Scattering (GISANS) data showed a peak corresponding between the distance between the droplets. In the GISANS there was also an additional peak which is attributed to the internal structure of the droplets. These samples were deposited onto silicon gratings with grooves $40\mu m$ wide (50 $\mu m$ period and 26nm

deep). After annealing of the grating dewetting and island formation was observed which was characterised by AFM.

Both the specular and off-specular scattering was measured for a bare grating and one containing the polymer. For the grating structure a series of features are observed, these are simply due to the grating in-plane period (d) and the modulation with the grooves placed perpendicular to the neutron beam in $Q_x = \frac{2\pi n}{d} = \frac{\pi n}{\lambda}(\theta_i^2 - \theta_f^2)$ of the Bragg ridges. As $\theta_i$ is fixed these trace out curved trajectories in $\theta_f - \lambda$ space (with the exception of the specular beam n=0) and as we know this relationship of the phase along these curves we can constrain the fits to equation 2 and extract the polarisation $P_0$.

Shown in figure 4 is an example plot from such analysis showing the echo polarisation as a function of wavelength for a pole shoe angle ($\theta_0$) of 50° (hence the spin echo length $z = c_{se}\lambda^2$ with $c_{se}/cot(\theta_0) = 2551nm^{-1}$). In all cases we compare with the specular beam from the bare grating. As expected with the grating grooves parallel to the spin-echo encoding direction there is no modification in the polarisation from that of the bare patterned substrate. The results are rather unpromising as they show no additional features from the dewetted polymer islands. In all cases the echo polarisation agrees with that determined from the specular ridge.

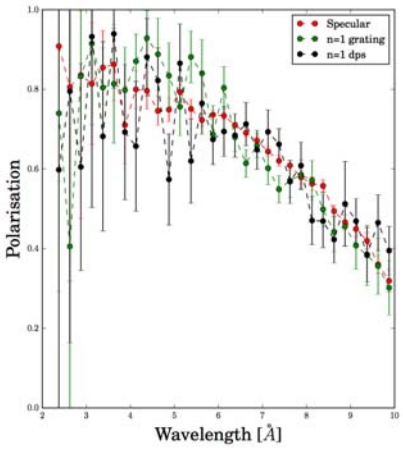


**Figure 4.** Spin Echo polarisation ($P_{se}$) as a function of wavelength for the n=1 reflection as labelled and the specular signal and a coated and uncoated grating with the dewetted polymer.

## 5. Discussion and conclusions

The work presented here shows that the RF gradient coils used in this work have small magnetic field inhomogeneities, however these can be corrected for and simultaneous measurement over a large angular coverage achieved, if the echo polarisation is determined. However despite this approach no additional scattering was observed from the dewetted polymers. The AFM measurements suggest that there are similar structures to those observed by Vorobiev *et al.* [21]. Also the question arises as to why SERGIS worked in the Parnell *et al* [20] investigation. Vorobiev at al used a 5.5 Åbeam of 30 x 2mm$^2$ around $0.5\alpha_c$ to $3\alpha_c$, where $\alpha_c$ is the silicon critical edge.

One key difference between the work of Parnell *et al* and Vorobiev *et al* is the amount of material in the beam. In Vorobiev's work the islands are $\approx 10nm$ tall whereas in Parnell's they are $\approx 1\mu m$, a factor 100 increase in material. This may explain the success of the Parnell study. However the overriding question is whether the technique can be applied in general to the investigation of buried in-plane structures. The quoted flux for Eva [25] is $\approx 9.8 \times 10^5 ns^{-1}cm^{-2}$, however no statement is made in the reference as to whether this is polarised and unpolarised. However just simply increasing the flux may not help as the visibility of the SERGIS signal is dependent upon measuring a small signal on a larger signal as explained in the introduction.

Hence it may be that only within the Yoneda region such a signal is visible as illustrated by Vorobiev *et al.* [21] in figure 4. If that is so then such experiments should be possible at ESS, if the integrated flux is of the same order of magnitude as that of the ILL. For one glancing angle, the monochromatic setup at ILL measures the off-specular intensity of one point of the Yoneda wing whilst the tof method measures the whole Yoneda wing simultaneously.

To conclude we remark that using the polarisation echo recovery method here we are able to correct for spatial aberrations in the magnetic field integral, such an approach is necessary when simultaneously looking over a range of scattering angles.

## 6. Acknowledgements

We would like to acknowledge discussions with Roger Pynn (Indiana), Andrew Parnell (Sheffield) A.Vorobiev. We acknowledge the STFC proposals RB1010439 and RB1510189 and thank Peter Muller-Buschbaum (TU Munich) for the polymer samples and Henk van Zeijl (TU Delft).

## 7. References

[1] Mezei F 1972 *Zeitscrihft Fur Physik* **255** 146
[2] Keller T, Gähler R, Kunze H and Golub R 1995 *Neutron News* **6** 16–17
[3] Rekveldt M T 1996 *Nuclear Instruments and Methods in Physics Research Section B: Beam Interactions with Materials and Atoms* **114** 366–370
[4] van Oossanen M, Kraan W H, Bouwman W G and Rekveldt M T 2000 *Physica B: Condensed Matter* **276–278** 134–135
[5] Pynn R, Lee W T, Stonaha P, Shah V R, Washington A L, Kirby B J, Majkrzak C F and Maranville B B 2008 *Rev Sci Instrum* **79** 063901
[6] Parnell S R, Washington A L, Li K, Yan H, Stonaha P, Li F, Wang T, Walsh A, Chen W C, Parnell A J, Fairclough J P A, Baxter D V, Snow W M and Pynn R 2015 *Review of Scientific Instruments* **86** 023902
[7] Li F, Parnell S R, Hamilton W A, Maranville B B, Wang T, Semerad R, Baxter D V, Cremer J T and Pynn R 2014 *Review of Scientific Instruments* **85** –
[8] Li F, Parnell S R, Bai H, Yang W, Hamilton W A, Maranville B B, Ashkar R, Baxter D V, Cremer J T and Pynn R 2016 *Journal of Applied Crystallography* **49** 55–63
[9] Li F, Parnell S R, Wang T, Baxter D V and Pynn R 2016 *Journal of Physics: Conference Series* **711** 012015
[10] Plomp J, de Haan V O, Dalgliesh R M, Langridge S and van Well A A 2007 *Thin Solid Films* **515** 5732–5735
[11] Parnell S R, Washington A L, Parnell A J, Walsh A, Dalgliesh R M, Li F, Hamilton W A, Prevost S, Fairclough J P A and Pynn R 2016 *Soft Matter* **12**(21) 4709–4714
[12] Andersson R, Bouwman W G, Luding S and de Schepper I M 2008 *Granular Matter* **10** 407–414
[13] Tromp R H and Bouwman W G 2007 *Food Hydrocolloids* **21** 154–158
[14] Rekveldt M T, Keller T and Golub R 2001 *EPL (Europhysics Letters)* **54** 342
[15] Repper J, Keller T, Hofmann M, Krempaszky C, Petry W and Werner E 2010 *Acta Materialia* **58** 3459–3467
[16] Major J, Dosch H, Felcher G, Habicht K, Keller T, te Velthuis S, Vorobiev A and Wahl M 2003 *Physica B: Condensed Matter* **336** 8 – 15
[17] Pynn R, Fitzsimmons M R, Rekveldt M T, Major J, Fritzsche H, Weller D and Johns E C 2002 *Review of Scientific Instruments* **73** 2948–2957
[18] De Haan V O, Plomp J, Bouwman W G, Trinker M, Rekveldt M T, Duif C P, Jericha E, Rauch H and Van Well A A 2007 *Journal of Applied Crystallography* **40** 151–157
[19] Ashkar R, Stonaha P, Washington A L, Shah V R, Fitzsimmons M R, Maranville B, Majkrzak C F, Lee W T, Schaich W L and Pynn R 2010 *Journal of Applied Crystallography* **43** 455–465
[20] Parnell A J, Dalgliesh R M, Jones R A L and Dunbar A D F 2013 *Applied Physics Letters* **102**
[21] Vorobiev A, Major J, Dosch H, Müller-Buschbaum P, Falus P, Felcher G P and te Velthuis S G E 2011 *The Journal of Physical Chemistry B* **115** 5754–5765
[22] Yoneda Y 1963 *Physical Review* **131** 2010–2013
[23] Farago B 2003 *Neutron Spin Echo Spectroscopy: Basics, Trends and Applications* Springer Lecture Notes in Physics (Berlin, Heidelberg: Springer)
[24] Müller-Buschbaum P, Bauer E, Wunnicke O and Stamm M 2005 *Journal of Physics: Condensed Matter* **17** S363
[25] *Ill Yellow Book* (Ill)